Core-Collapse Supernovae: Explosion Dynamics, Neutrinos and Gravitational Waves

Bernhard Müller[1], *Hans-Thomas Janka*[1], *Andreas Marek*[1], *Florian Hanke*[1], *Annop Wongwathanarat*[1], *Ewald Müller*[1]

[1]Max-Planck-Institut für Astrophysik, Karl-Schwarzschild-Str. 1, 85748 Garching, Germany

DOI: http://dx.doi.org/10.3204/DESY-PROC-2011-03/mueller

The quest for the supernova explosion mechanism has been one of the outstanding challenges in computational astrophysics for several decades. Simulations have now progressed to a stage at which the solution appears close and neutrino and gravitational wave signals from self-consistent explosion models are becoming available. Here we focus one of the recent advances in supernova modeling, the inclusion of general relativity in multi-dimensional neutrino hydrodynamics simulations, and present the latest simulation results for an $11.2M_\odot$ and a $15M_\odot$ progenitor. We also mention 3D effects as another aspect in supernova physics awaiting further, more thorough investigation.

1 Introduction

Massive stars end their lives as a core-collapse supernova (SN), a violent event that involves the collapse of the iron core of the progenitor to a proto-neutron star and the subsequent expulsion of the outer layers of the star with a kinetic energy on the order of 10^{51} erg, which is associated with a spectacularly bright optical display. Currently, there is still no final consensus on the supernova explosion mechanism that operates in the optically obscured supernova core, and a number of competing ideas are under discussion. The delayed neutrino-driven mechanism [1, 2], which relies on neutrino energy deposition in the gain region to revive the stalled shock, remains the most promising candidate, provided that the efficiency of neutrino heating can be sufficiently enhanced by multi-dimensional hydrodynamical instabilities such as convection and the so-called standing accretion shock instability SASI [3, 4]. This mechanism has worked successfully in several recent 2D simulations [5, 6, 7] (some of which appeared to be only marginally successful [6]), but has failed in others [8, 9]. Alternatives to the neutrino-driven mechanism have also been proposed, such as the acoustic mechanism [8, 9] (whose viability has been called into question by [10], however), magnetohydrodynamically driven supernovae [11, 12], and explosions triggered by a QCD phase transition [13].

As the "engine" driving this explosion is not directly accessible by classical, photon-based astronomical observations, our understanding of the supernova explosion mechanism has largely rested on numerical simulations in the past ever since the pioneering work of [14]. Over the years, a variety of ambitious numerical approaches has been developed to cope with the challenging interplay of neutrino transport, multidimensional hydrodynamics, general relativity (GR), neutrino physics, and nuclear physics in the supernova problem. The currently most advanced models rely on sophisticated multi-group neutrino transport schemes (e.g. ray-by-ray

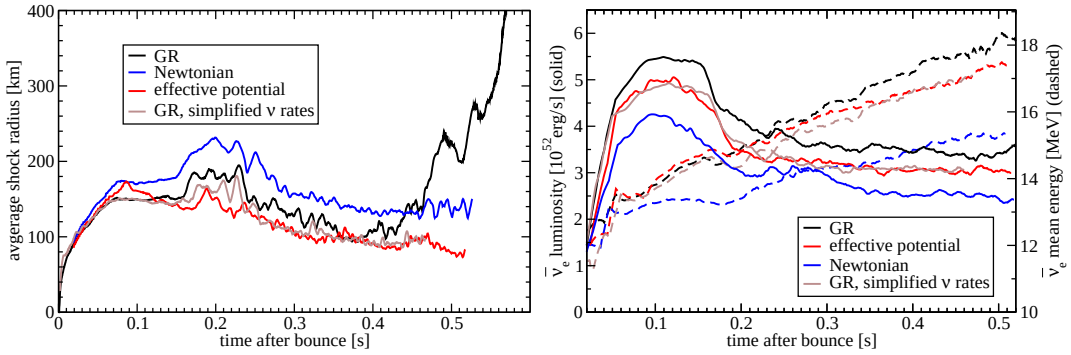

Figure 1: (color online) Left: Average shock radius for the $15M_\odot$ model as obtained in GR with our best set of opacities (black curve) and with simplified neutrino rates (light brown curve), in the purely Newtonian approximation (blue), and with an effective gravitational potential (red). Right: Electron antineutrino luminosities (solid) and mean energies (dashed) at the gain radius for these three cases.

variable Eddington factor transport [15, 16], ray-by-ray-diffusion [7], 2D multi-angle transport without energy bin coupling [17], or the isotropic diffusion source approximation [18]) with different strengths and weaknesses, and there have only been very tentative attempts to venture forth to 3D models with these methods [7, 19]. Elements missing or only partially included in current state-of-the-art-models, such as 3D effects (whose potential is presently being debated [20, 19, 21]) or general relativity may hold the key to a better understanding of the explosion mechanism. Moreover, an improved treatment of such as yet poorly explored aspects is also indispensable for accurate predictions of the neutrino and gravitational wave signal – the only *observables* that directly probe the dynamics in the supernova core.

Among the aspects that have not yet been thoroughly investigated in self-consistent multi-D neutrino hydrodynamics simulations of core-collapse supernovae, our group has recently begun to study the influence of GR in more detail. Although the importance of relativistic effects in core-collapse supernovae (due to the compactness of the proto-neutron star and the occurrence of high velocities) has long been recognized an demonstrated [22], the combination of GR hydrodynamics and multi-group neutrino transport has long been feasible only in spherical symmetry [22, 23, 24]. With the relativistic generalization of the ray-by-ray variable Eddington factor method [25] used in our neutrino hydrodynamics code VERTEX, we are now able to present first results about the impact of GR on the explosion dynamics and, in particular, the neutrino and gravitational wave emission in axisymmetric (2D) supernova models.

2 General Relativistic Effects in Multi-Dimensional Supernova Models

Our group has recently conducted relativistic supernova simulations for progenitors with $11.2M_\odot$ [26] and $15M_\odot$ [27] well into the explosion phase, which were supplemented by three additional runs for the $15M_\odot$ star. In order to estimate the magnitude of GR effects, two complementary models were computed using either the purely Newtonian approximation or the "effective po-

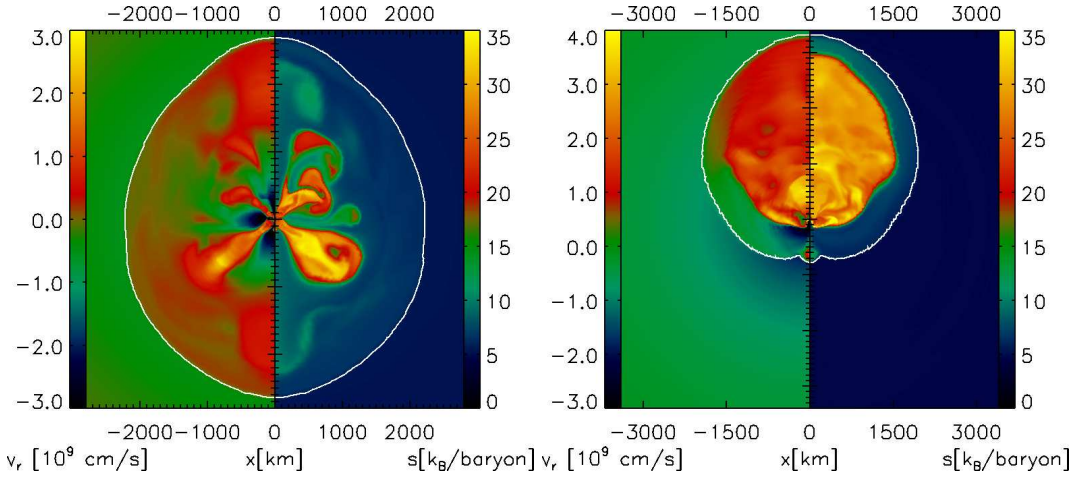

Figure 2: (color online) Explosion geometry for the GR simulations of the $11.2M_\odot$ (left panel, almost spherical shock) and the $15M_\odot$ progenitor (right panel, strong dipolar shock deformation) 658 ms and 745 ms after bounce, respectively. The left and right half of the panels show the electron fraction Y_e and the entropy s, respectively, and the shock is indicated as a white curve.

tential" approach [28], which has long been the only means of including some GR corrections in multi-D neutrino hydrodynamics simulations. In addition, we also calculated a model with a simplified set of neutrino opacities (neglecting the effects of recoil, high-density correlations and weak magnetism in neutrino-nucleon reactions and ignoring reactions between different neutrino flavors), which serves to illustrate the importance of the neutrino microphysics for the dynamics in the supernova core and provides a scale of reference for the GR effects. As a marginal case close to the threshold between explosion and failure [6], the $15M_\odot$ progenitor is ideally suited for such a comparative analysis.

Interestingly, we find that among the $15M_\odot$ models, the GR run with improved rates is the only one to develop an explosion with shock revival occurring some 450 ms after bounce (Fig. 1), indicating the relevance of both GR effects *and* of the neutrino microphysics. The different evolution of the three models with a different treatment of gravity is a consequence of the different compactness and surface temperature of the proto-neutron star, which leads to a clear hierarchy of the electron neutrino and antineutrino luminosities and mean energies (which determine the heating conditions) between the three cases (cp. [22, 29, 25] for this effect in 1D simulations) as illustrated by Fig. 1 for the electron antineutrinos, where the enhancement in GR is most pronounced. The beneficial effect of higher local heating rates as compared to the Newtonian case is, however, counterbalanced by the faster advection of material through the gain layer around a more compact proto-neutron star in the effective potential run, but in the GR case, the enhanced heating is strong enough to overcome this adverse effect.

It is noteworthy that the neutrino emission and the shock evolution are similarly sensitive to the neutrino interaction rates (in agreement with the findings of [30, 7]). In the run with improved microphysics, weak magnetism and nucleon correlations lower the opacities for $\bar{\nu}_e$, shift the neutrinosphere into deeper and hotter regions of the proto-neutron star surface [31], and thus result in harder $\bar{\nu}_e$ spectra (by up to ~ 1 MeV during the late phases) and increased $\bar{\nu}_e$

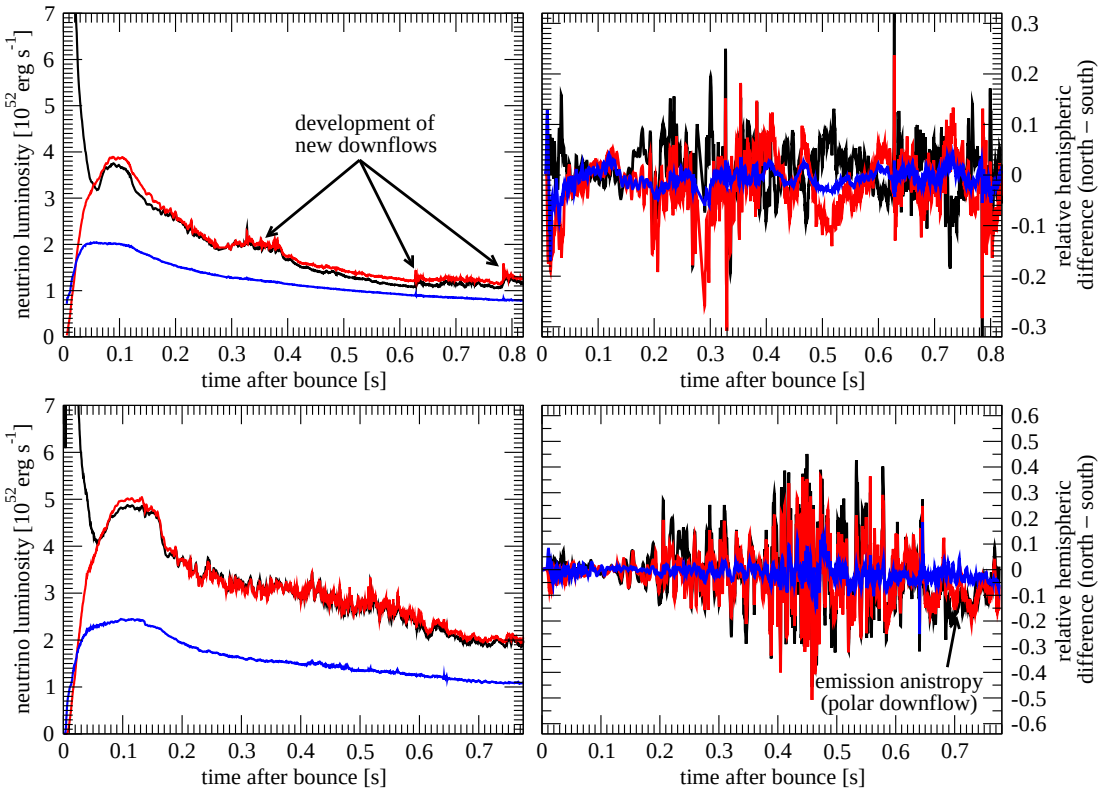

Figure 3: (color online) Left panels: Neutrino luminosities (defined as the total angle-integrated neutrino flux from the supernova) for the relativistic $11.2M_\odot$ (top) and $15M_\odot$ (bottom) models. Right panels: Relative differences of the angle-integrated neutrino fluxes $L_{\rm north}$ and $L_{\rm south}$ in the northern and southern hemisphere, computed as $2(L_{\rm north}-L_{\rm south})/(L_{\rm north}+L_{\rm south})$. Black, red, and blue curves are used for ν_e, $\bar{\nu}_e$, and $\nu_{\mu/\tau}$, respectively.

luminosities, which also allows for more efficient heating in the gain layer. Neglecting possible effects of flavor conversion and MSW, this would also imply somewhat higher detection rates for $\bar{\nu}_e$ (by $\sim 15\%$).

3 Neutrino and Gravitational Wave Signals from Supernovae

Both the $11.2M_\odot$ and the $15M_\odot$ models have been evolved well into the post-explosion phase until ~ 0.8 s after bounce, and thus provide a good illustration of the impact of multi-dimensional effects on the neutrino and gravitational wave signal during the different stages of the evolution. Prior to the onset of the explosion the neutrino luminosities of both models (Fig.3, left panels) are characterized by the familiar large contribution of the accretion luminosity for ν_e and $\bar{\nu}_e$. As soon as the SASI starts to grow vigorously, we also observe the strong angle-dependent time

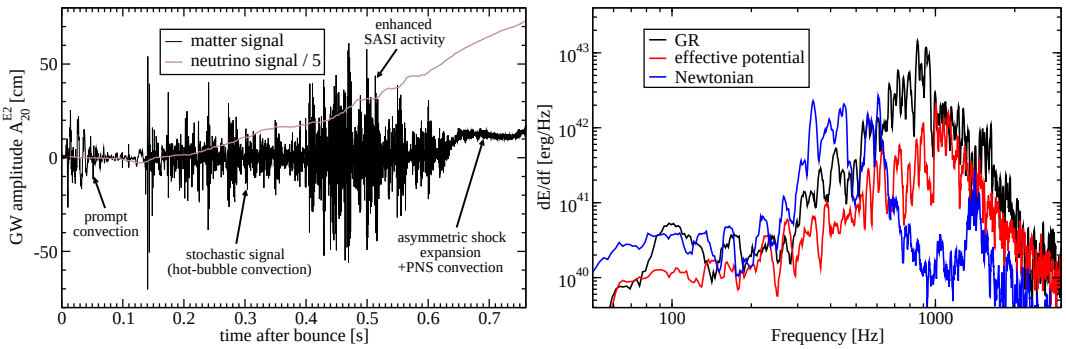

Figure 4: (color online) Left: Matter (black) and neutrino (light brown) gravitational wave signals for the general relativistic $15M_\odot$ explosion model. Right: Influence of the treatment of gravity (black: GR hydro, red: Newtonian hydro + effective potential, blue: purely Newtonian) on the gravitational wave energy spectrum for the first 500 ms of the post-bounce evolution of the $15M_\odot$ progenitor.

variations in the neutrino flux (particularly in ν_e and $\bar{\nu}_e$, see Fig. 3, right panels) that have been discussed in [17, 32, 33, 34] and can potentially be used to extract the frequencies of the SASI from the neutrino signal using detectors with high temporal resolution such as Icecube [33]. In our simulations, these fluctuations are present in similar strength as in Newtonian and effective potential models [17, 32, 34] with the hemispheric flux fluctuating by several tens of percent; and the dominant frequencies (45 Hz and 75 Hz for the $\ell = 1$ and $\ell = 2$ mode) are in excellent agreement with [32, 33].

It is interesting to note that our results suggest that the neutrino signal changes its character only gradually over several hundreds of milliseconds after the onset of the explosion. The temporal fluctuations are actually strongest during the first ~ 200 ms after shock revival, and the luminosities of ν_e and $\bar{\nu}_e$ do not show any abrupt decline correlated with the time of the explosion. This behavior is in marked contrast to the abrupt drop in the ν_e and $\bar{\nu}_e$ luminosities in 1D models with artificial explosions [35], and is due to the fact that quite large accretion rates can still be maintained through the downflows at late times in multi-dimensional models (Fig. 2). As long as the shock does not expand too rapidly, new downflows may still form and channel fresh material into the cooling region (see [6], as in the case of the $11.2M_\odot$ progenitor, which leads to noticeable "bumps" in the neutrino luminosity (Fig. 3, top left panel). For the $15M_\odot$ progenitor, an even higher accretion luminosity can be maintained continuously because of the presence of a stable polar downflow in an extremely asymmetric explosion geometry (Fig. 2). With a single downflow, the neutrino emission exhibits a strong directional dependence with sustained hemispheric flux differences of up to several tens of percent (Fig. 3). On the other hand, the strong high-frequency fluctuations subside during the late phases as the expansion of the shock quenches further SASI activity. The neutrino signal thus still reflects the dynamical evolution of explosion models in multi-D, albeit in a form very different from artificial 1D explosions.

Naturally, the determination of gravitational wave signals has also been among the major goals of the simulations with the relativistic version of VERTEX. Qualitatively, we obtain similar waveforms as computed in the Newtonian or effective potential approximation [32, 36, 37]

with clearly distinct phases in the signal corresponding to the dynamics (Fig. 4, cp. with ref. [36]). Shortly after bounce, prompt convection and early SASI activity produce a low-frequency, quasi-periodic signal, which is followed by a more quiescent period until hot-bubble convection and strengthening SASI sloshing motions gives rise to a stochastic signal with typical frequencies rising from 500 Hz to over 1000 Hz during a phase of $\sim$ 200 ms around shock revival revival, when gravitational wave emission is strongest. Afterwards, proto-neutron star convection becomes the dominant source of high-frequency gravitational waves. In the case of the $15M_{\odot}$ progenitor with a rather extreme explosion geometry, asymmetric shock expansion and neutrino emission also give rise to a monotonously rising "tail signal" which contributes somewhat to the low-frequency part of the spectrum. Despite the qualitative similarities of waveforms in GR and the Newtonian approximation, GR effects have a considerable impact on the power spectrum, however. The integrated signal for the first 500 s (Fig. 4) peaks at considerably higher frequencies in GR ($\sim$ 900 Hz) compared to the purely Newtonian case ($\sim$ 500 Hz). On the other hand, the effective potential approximation even overestimates the peak frequency ($\sim$ 1100 Hz), because the lower proto-neutron star surface temperature leads to a higher Brunt-Väisälä frequency and therefore to a more abrupt braking of convective bubbles at the lower boundary of the hot-bubble convection region (cp. with the interpretation of the characteristic frequencies given in [36]).

4 Outlook – 3D Supernova Modeling

The results presented here demonstrate that both GR effects and variations in the neutrino microphysics have a significant impact on the neutrino emission and, consequently, and on the dynamics in the supernova core. As illustrated by the marginal $15M_{\odot}$ progenitor, a detailed and sophisticated treatment of gravity and neutrino interactions can very well be crucial for the success of the neutrino-driven explosion mechanism. Such improvements in the models also bring up the perspective of reliable, non-parametrized predictions for the neutrino and gravitational wave signal *beyond* the accretion phase (cp. also [37]), whose salient features have been pointed out in the last section.

One of the major limitations of the models discussed here is their restriction to axisymmetry, which presently remains a necessary compromise for simulations with the most advanced multi-group neutrino transport methods. In the meantime, 3D effects can already be explored with the help of parametrized approaches and cheaper approximative methods to gain insights into their potentially important role for the explosion mechanism [20, 19, 21] and the expected changes in the neutrino and gravitational wave signals [38]. On the background of the strong sensitivity of the heating conditions on the neutrino treatment, conclusions about the implications of 3D effects for the viability of the neutrino-driven mechanism can only be drawn with some caution, however. Recent studies by [19] and by our own group [21] have indeed demonstrated that models do not necessarily explode more easily in 3D than in 2D [19, 21], and have rather pointed out issues that require further investigation, such as the role of feedback effects of convection and the SASI on the neutrino emission[19, 21], dimensionality-dependent resolution effects due to the different direction of the turbulent cascade [21], and the growth and saturation of the SASI in 3D [21].

While the influence of the dimensionality on the explosion conditions remains a controversial topic, the gravitational wave [39, 40, 41, 42] and neutrino signatures of non-radial hydrodynamic instabilities developing during the post-bounce phase will undoubtedly be affected by going from

2D to 3D. First predictions based on models with simplified semi-parametrized neutrino transport have recently become available [38], and suggest that the lack of a preferred direction in 3D and weaker activity of the $l = 1$ SASI sloshing mode reduce both the gravitational wave amplitude and the fast temporal variations of the neutrino signal by a factor of several. Even these findings are still subject to uncertainties about the dynamics in the supernova core (in particular concerning the behavior of the SASI in 3D), and in the end, accurate signal predictions will also require self-consistent simulations with at least the same level of sophistication as currently available in 2D.

Acknowledgments

This work was supported by the Deutsche Forschungsgemeinschaft through the Transregional Collaborative Research Centers SFB/TR 27 "Neutrinos and Beyond" and SFB/TR 7 "Gravitational Wave Astronomy" and the Cluster of Excellence EXC 153 "Origin and Structure of the Universe" (http://www.universe-cluster.de). The simulations of the MPA core-collapse group were performed on the IBM p690 of the Computer Center Garching (RZG), the NEC SX-8 at the HLRS in Stuttgart (within the SUPERN project), the Juropa Cluster at the John von Neumann Institute for Computing (NIC) in Jülich (partially through a DECI-6 grant of the EU), and on the IBM p690 at Cineca in Italy through a DECI-5 grant of the DEISA initiative.

References

[1] J. R. Wilson, Supernovae and Post-Collapse Behavior, in *Numerical Astrophysics*, edited by J. M. Centrella, J. M. Leblanc, and R. L. Bowers, pp. 422–434, 1985.

[2] H. A. Bethe and J. R. Wilson, Astrophys. J. **295**, 14 (1985).

[3] J. M. Blondin, A. Mezzacappa, and C. DeMarino, Astrophys. J. **584**, 971 (2003).

[4] T. Foglizzo, L. Scheck, and H.-T. Janka, Astrophys. J. **652**, 1436 (2006).

[5] R. Buras, H.-T. Janka, M. Rampp, and K. Kifonidis, Astron. Astrophys. **457**, 281 (2006).

[6] A. Marek and H.-T. Janka, Astrophys. J. **694**, 664 (2009).

[7] S. W. Bruenn *et al.*, ArXiv e-prints (2010), arXiv:1002.4914.

[8] A. Burrows, E. Livne, L. Dessart, C. D. Ott, and J. Murphy, Astrophys. J. **640**, 878 (2006).

[9] A. Burrows, E. Livne, L. Dessart, C. D. Ott, and J. Murphy, Astrophys. J. **655**, 416 (2007).

[10] N. N. Weinberg and E. Quataert, Mon. Not. R. Astron. Soc.**387**, L64 (2008).

[11] S. Akiyama, J. C. Wheeler, D. L. Meier, and I. Lichtenstadt, Astrophys. J. **584**, 954 (2003).

[12] A. Burrows, L. Dessart, E. Livne, C. D. Ott, and J. Murphy, Astrophys. J. **664**, 416 (2007).

[13] I. Sagert *et al.*, Physical Review Letters **102**, 081101:1 (2009).

[14] S. A. Colgate and R. H. White, Astrophys. J. **143**, 626 (1966).

[15] M. Rampp and H.-T. Janka, Astron. Astrophys. **396**, 361 (2002).

[16] R. Buras, M. Rampp, H.-T. Janka, and K. Kifonidis, Astron. Astrophys. **447**, 1049 (2006).

[17] C. D. Ott, A. Burrows, L. Dessart, and E. Livne, Astrophys. J. **685**, 1069 (2008).

[18] M. Liebendörfer, S. C. Whitehouse, and T. Fischer, Astrophys. J. **698**, 1174 (2009).

[19] T. Takiwaki, K. Kotake, and Y. Suwa, ArXiv e-prints (2011), arXiv:1108.3989.

[20] J. Nordhaus, A. Burrows, A. Almgren, and J. Bell, Astrophys. J. **720**, 694 (2010).

[21] F. Hanke, A. Marek, B. Müller, and H.-T. Janka, ArXiv e-prints (2011), arXiv:1108.4355.

[22] S. W. Bruenn, K. R. De Nisco, and A. Mezzacappa, Astrophys. J. **560**, 326 (2001).

[23] S. Yamada, H.-T. Janka, and H. Suzuki, Astron. Astrophys. **344**, 533 (1999).

[24] M. Liebendörfer *et al.*, Astrophys. J. Suppl. **150**, 263 (2004).

[25] B. Müller, H.-T. Janka, and H. Dimmelmeier, Astrophys. J. Suppl. **189**, 104 (2010).

[26] S. E. Woosley, A. Heger, and T. A. Weaver, *Rev. Mod. Phys.* **74**, 1015 (2002).

[27] S. E. Woosley and T. A. Weaver, Astrophys. J. Suppl. **101**, 181 (1995).

[28] A. Marek, H. Dimmelmeier, H.-T. Janka, E. Müller, and R. Buras, Astron. Astrophys. **445**, 273 (2006).

[29] M. Liebendörfer, M. Rampp, H.-T. Janka, and A. Mezzacappa, Astrophys. J. **620**, 840 (2005).

[30] M. Rampp, R. Buras, H.-T. Janka, and G. Raffelt, Core-collapse supernova simulations: variations of the input physics, in *Nuclear Astrophysics*, edited by W. Hillebrandt & E. Müller, pp. 119–125, 2002.

[31] C. J. Horowitz, Phys. Rev. D **65**, 043001 (2002).

[32] A. Marek, H.-T. Janka, and E. Müller, Astron. Astrophys. **496**, 475 (2009).

[33] T. Lund, A. Marek, C. Lunardini, H.-T. Janka, and G. Raffelt, Phys. Rev. D **82**, 063007 (2010).

[34] T. D. Brandt, A. Burrows, C. D. Ott, and E. Livne, Astrophys. J. **728**, 8 (2011).

[35] T. Fischer, S. C. Whitehouse, A. Mezzacappa, F. Thielemann, and M. Liebendörfer, Astron. Astrophys. **517**, A80+ (2010).

[36] J. W. Murphy, C. D. Ott, and A. Burrows, Astrophys. J. **707**, 1173 (2009).

[37] K. N. Yakunin *et al.*, Classical and Quantum Gravity **27**, 194005 (2010).

[38] E. Müller, H.-T. Janka, and A. Wongwathanarat, ArXiv e-prints (2011), arXiv:1106.6301.

[39] S. Scheidegger, T. Fischer, S. C. Whitehouse, and M. Liebendörfer, Astron. Astrophys. **490**, 231 (2008).

[40] K. Kotake, W. Iwakami, N. Ohnishi, and S. Yamada, Astrophys. J. **697**, L133 (2009).

[41] S. Scheidegger, R. Käppeli, S. C. Whitehouse, T. Fischer, and M. Liebendörfer, Astron. Astrophys. **514**, A51+ (2010).

[42] K. Kotake, W. Iwakami-Nakano, and N. Ohnishi, Astrophys. J. **736**, 124 (2011).